Published online February 18, 2004

Nucleic Acids Research, 2004, Vol. 32, No. 3 ***1177–1183***
DOI: 10.1093/nar/gkh288

Identification of NH...N hydrogen bonds by magic angle spinning solid state NMR in a double-stranded RNA associated with myotonic dystrophy

Jörg Leppert, Carl R. Urbinati[1], Sabine Häfner, Oliver Ohlenschläger, Maurice S. Swanson[1], Matthias Görlach and Ramadurai Ramachandran*

Abteilung Molekulare Biophysik/NMR-Spektroskopie, Institut für Molekulare Biotechnologie, 07745 Jena, Germany and [1]Department of Molecular Genetics and Microbiology, Powell Gene Therapy Center, University of Florida, College of Medicine, 1600 SW Archer Road, Gainesville, FL 32610-0266, USA

Received December 4, 2003; Revised and Accepted January 27, 2004

ABSTRACT

RNA plays a central role in biological processes and exhibits a variety of secondary and tertiary structural features that are often stabilized via hydrogen bonds. The distance between the donor and acceptor nitrogen nuclei involved in NH...N hydrogen bonds in nucleic acid base pairs is typically in the range of 2.6–2.9 Å. Here, we show for the first time that such spatial proximity between ^{15}N nitrogen nuclei can be conveniently monitored via magic angle spinning solid state NMR on a uniformly ^{15}N-labelled RNA. The presence of NH...N hydrogen bonds is reflected as cross-peaks between the donor and acceptor nitrogen nuclei in 2D ^{15}N dipolar chemical shift correlation spectra. The RNA selected for this experimental study was a CUG repeat expansion implicated in the neuromuscular disease myotonic dystrophy. The results presented provide direct evidence that the CUG repeat expansion adopts a double-stranded conformation.

INTRODUCTION

A variety of secondary and tertiary structural features are exhibited by RNAs that are involved in a multitude of biological processes (1). Previously, the structural characterization of RNA has been undertaken mainly via X-ray crystallography and solution state NMR. Efficient isotopic labelling techniques, high-field spectrometers and multidimensional FT NMR have made RNA structure elucidation possible, and structural characteristics of a variety of interesting RNA and RNA–protein complexes have been elucidated via solution state NMR (2–6). The prerequisite for any NMR-based structure determination is the sequence-specific assignment of resonances, and homo- and heteronuclear chemical shift correlation experiments are commonly employed in this context. Many of the heteronuclear techniques used for RNA resonance assignments in the solution state require radiofrequency (RF) pulse trains with large interpulse delays (7). For large RNAs with correspondingly broad NMR linewidths, the efficacy of solution state NMR techniques for structure determination is considerably reduced. On the other hand, solid state NMR (ssNMR) poses no such size limitations. The linewidth observed in the solid state is not dependent on the size of the molecule. Additionally, large dipolar couplings permit efficient homo- and heteronuclear coherence transfers.

Owing to the increased resolution and sensitivity obtainable, magic angle spinning (MAS) ssNMR is the method of choice for the study of polycrystalline specimens. Although weak dipolar couplings between low γ nuclei are normally averaged out under MAS, a variety of homo- and heteronuclear dipolar recoupling techniques have been introduced recently (8–10). Besides permitting the generation of chemical shift correlation data, dipolar recoupling experiments may also be used to obtain structural constraints such as distances and torsion angles. As with solution state NMR, it is possible to employ the distance geometry approach to generate an ensemble of structures that are consistent with ssNMR derived distance constraints. Such an approach has been elegantly demonstrated by Castellani *et al*. (11) in their MAS ssNMR study of the SH3 domain of α-spectrin. However, MAS ssNMR has not been employed in structural studies of RNA to date. As mentioned above, assignment of RNA resonances is the critical first step for any ssNMR-based structure determination. Duplex regions, characterized by hydrogen bonding between complementary bases, are commonly found in RNA. In solution state NMR, NH...N hydrogen bonds in canonical and non-canonical base pairs of RNA are identified by HNN-COSY (12,13). This experiment makes use of the scalar coupling interaction to correlate the hydrogen-bonded nitrogen nuclei and the efficacy of the approach has been demonstrated in a variety of systems (14). A similar approach, which correlates the imino donor ^{15}N nucleus and the

*To whom correspondence should be addressed. Tel: +49 3641 656222 or +49 3641 656220; Fax: +49 3641 656225; Email: raman@imb-jena.de
Correspondence may also be addressed to Matthias Görlach. Email: mago@imb-jena.de

corresponding acceptor ^{15}N nucleus of a complementary base, should be useful in ssNMR studies of ^{15}N-labelled RNA. As the scalar coupling between hydrogen-bonded nitrogen nuclei is typically small, it is necessary to employ large mixing times to induce coherence transfer and to obtain correlation peaks with measurable signal intensities. Such weak scalar coupling based experiments in the solid state are generally difficult to implement due to technical difficulties (e.g. the application of a high-power ^{1}H decoupling field for durations that are much longer than the typical MAS NMR probe specifications). Additionally, significant signal intensity losses arising from transverse relaxation processes may also be encountered. On the other hand, in solid state one can take advantage of the fact that in NH...N hydrogen bonds the nitrogen nuclei are spatially proximal, with typical N–N distances being in the range of 2.9–2.6 Å corresponding to a dipolar coupling strength (D_{NN}) of ~50–70 Hz. Such spatial proximity of nitrogen nuclei, and hence the presence of hydrogen-bonded base pairs, can be monitored via MAS homonuclear dipolar correlation experiments.

Radiofrequency driven recoupling (RFDR) with longitudinal magnetization exchange (15,16) is one of the techniques that has found wide application for generating 2D MAS dipolar chemical shift correlation spectra in biological systems (17–21). RFDR is a zero-quantum recoupling sequence and involves the application of rotor synchronized 180° pulses for dipolar recoupling. Recently, we have shown that superior performance can be obtained by employing adiabatic instead of the conventional rectangular inversion pulses in the RFDR sequence (22,23).

Since homonuclear ^{15}N dipolar correlation experiments on RNA have not been reported previously, we have evaluated numerically and experimentally the potential of RFDR with adiabatic pulses for obtaining ^{15}N dipolar correlation spectra in uniformly ^{15}N-labelled RNA. The numerical results presented here indicate that adiabatic inversion pulse driven ^{15}N magnetization exchange spectroscopy can lead to cross-peaks of measurable signal intensity between the imino donor nitrogen and the corresponding acceptor nucleus on the complementary base. We have also experimentally assessed the efficacy of these emerging techniques by performing ^{15}N dipolar correlation experiments on a 100 kDa RNA composed of 97 CUG repeats, or $(CUG)_{97}$. The experimental results show that MAS ^{15}N dipolar correlation experiments facilitate the identification of hydrogen-bonded base pairs.

CUG repeats of >50 have been implicated in the neuromuscular disease myotonic dystrophy type 1 (DM1) (24). A current model for DM1 pathogenesis suggests that these repeats fold into large and stable double-stranded (ds) RNA hairpins (25,26) with GC and UU base pairs that sequester the muscleblind (MBNL) proteins (27,28). Sequestration and loss of MBNL function leads to misregulation of alternative pre-mRNA splicing of a number of gene transcripts. For example, the major skeletal muscle chloride channel ClC–1 is mis-spliced in both human DM1 and mouse *Mbnl1*$\Delta^{E3/}\Delta^{E3}$ knockout muscle leading to loss of normal chloride conductance and muscle hyperexcitability (myotonia) (29,30). The experimental results presented here provide direct evidence that this $(CUG)_{97}$ RNA adopts a double-stranded conformation.

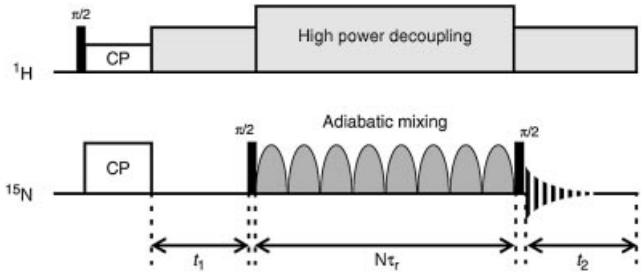

Figure 1. The RF pulse sequence employed for obtaining ^{15}N MAS dipolar chemical shift correlation spectra in the solid state. The sequence involves a conventional CP transfer from the ^{1}H nuclei to the ^{15}N nuclei under Hartmann–Hahn matching conditions. Following CP, the ^{15}N magnetization evolves for a period t_1 under the isotropic ^{15}N isotropic chemical shifts. The non-selective π/2 pulse applied at the end of t_1 restores the transverse nitrogen magnetization to the z axis. During the mixing period Nτ$_r$ dipolar recoupling is achieved via rotor-synchronized adiabatic inversion pulses with one pulse per rotor period and by employing the [p5m4] or [p5p7m4] phasing scheme (see text) for the inversion pulses. The final ^{15}N π/2 pulse returns the ^{15}N magnetization to the transverse plane for detection.

MATERIALS AND METHODS

RNA synthesis and sample preparation

$(CUG)_{97}$ was transcribed *in vitro* from the linearized plasmid pCTG coding for 97 consecutive CUG triplets (26). The $(CUG)_{97}$ RNA was purified in a uniformly ^{15}N-labelled form essentially as described (5). Purified $(CUG)_{97}$ was precipitated twice from 0.5 ml aqueous solution using 5 vol of 2% (w/v) $LiClO_4$ in acetone and redissolved in 1 ml water to a concentration of ~150 µM as estimated by UV absorption spectroscopy. Refolding of $(CUG)_{97}$ was achieved by adding 6 ml boiling H_2O, incubating this ~20 µM RNA solution at 95°C for 15 min and subsequent cooling to room temperature over 210 min. The RNA was subsequently lyophilized and ~85 nmol (8.5 mg) was placed into a 70 µl sealing cell that fits inside the MAS rotor (DOTY Scientific Inc., Columbia, USA). A high level of hydration was ensured by allowing the lyophilized RNA sample to equilibrate for 6 days in a sealed chamber with a water-saturated atmosphere. This sample was used for obtaining the first set of MAS ssNMR measurements and later dissolved in 50 µl of H_2O at pH 6.8 in order to carry out the experiments with the frozen solution. Also, from the same lyophilized RNA preparation, a 200 µM sample for solution state studies was prepared by dissolving the RNA in 20 mM sodium phosphate buffer pH 6.2 containing 40 mM KCl, 0.2 mM EDTA and 10% (v/v) D_2O (4). Denaturing gel electrophoresis in the presence of 7 M urea was performed according to standard procedures (31).

NMR spectroscopy and numerical simulations

MAS ssNMR experiments at a spinning speed of 7000 Hz were carried out at approximately –15°C on a 500 MHz wide-bore Varian ^{UNITY}*INOVA* ssNMR spectrometer equipped with a 5 mm DOTY supersonic triple resonance probe and a waveform generator for pulse shaping. Uniformly ^{15}N-labelled samples of $(CUG)_{97}$ were used for this investigation. Cross-polarization under Hartmann–Hahn matching conditions was employed and all spectra, unless mentioned otherwise, were collected under high-power ^{1}H decoupling

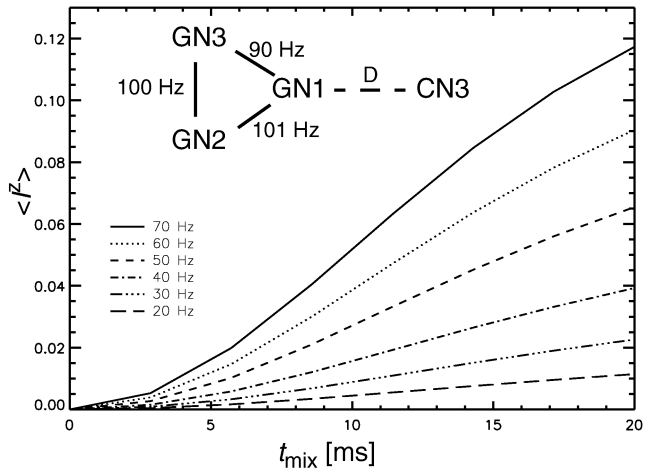

Figure 2. Simulated adiabatic inversion pulse driven longitudinal magnetization transfer characteristics. The plots show the magnitude of the transferred magnetization (normalized to the maximum transferable signal) at the CN3 nitrogen spin starting with z magnetization on spin GN1 at zero recoupling time. Considering a four-spin dipolar network, simulations were carried out at a spinning speed of 7000 Hz, with 'cagauss' adiabatic pulses (142 µs, 28.0 kHz γH_1, 50 kHz sweep width) (23,32) employing the [p5m4] phasing scheme and in time increments of 20 rotor periods. The resulting data points were interpolated to provide visual clarity. The plots show the dependence of the initial rate of build-up on the dipolar coupling strength D between the nuclei GN1 and CN3. Based on available internuclear distance data, the dipolar coupling strengths between the other nuclei were fixed at the values indicated. All simulations were carried out keeping the RF carrier on resonance with spin GN1, neglecting CSAs and employing resonance offsets $\Delta\delta$ of –3556, 818 and 2580 Hz for the GN2, GN3 and CN3 nuclei. The orientations of the dipolar vectors are taken from a SYBYL (Tripos Inc., San Louis, USA) generated A-form RNA duplex with a self-complementary CUGCUGCUG sequence and using the SIMMOL program to calculate the mutual orientations in an arbitrary molecular frame.

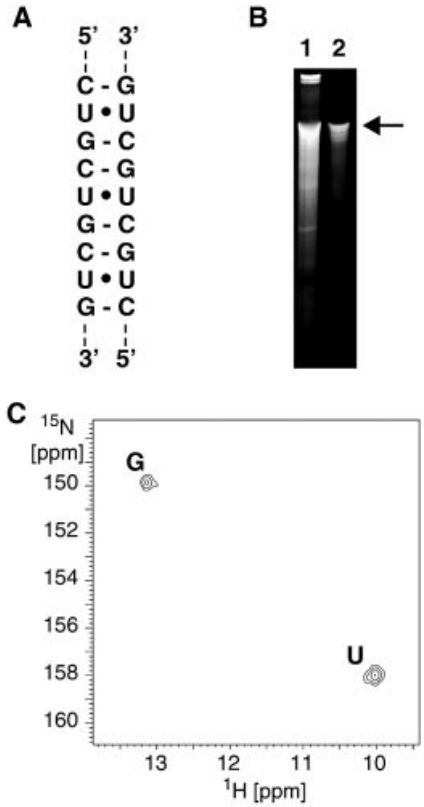

Figure 3. (**A**) Schematic representation of dsCUG. (**B**) Denaturing polyacrylamide gel electrophoresis of (1) the total ^{15}N-labelled RNA synthesized in a 15 ml *in vitro* transcription reaction and (2) $(CUG)_{97}$ RNA after purification and refolding. The arrow points to the full-length transcript. (**C**) A ^{1}H–^{15}N HSQC spectrum of a 200 µM $(CUG)_{97}$ sample taken at 15°C; G and U denote the cross-peaks of the imino groups of the G and U nucleotides of $(CUG)_{97}$.

(~90 kHz). Typical ^{1}H and ^{15}N 90° pulsewidths were 2.8 µs and 7.5 µs, respectively. ^{15}N dipolar chemical shift correlation experiments were carried out with one pulse per rotor period employing the RF pulse sequence shown in Figure 1. The adiabatic inversion pulses 'cagauss' (23,32) with 142 µs duration, $\omega_1(\text{max})/2\pi$ of ~28 kHz and a frequency sweep width of 50 kHz, as implemented in the Varian pulse-shaping software 'Pbox', were employed. For better preservation of longitudinal magnetizations at long mixing times the adiabatic inversion pulse phases were cycled as per the phasing scheme [p5m4] or [p5p7m4], where p5, p7 and m4 represent the phase cycles {0°, 240°, 240°, 60°, 0°}, {0°, 105°, 300°, 255°, 300°, 105°, 0°} and {0°, 0°, 180°, 180°}, respectively (33,34). Other details are given in the figure captions. Numerical simulations were carried out with the SIMPSON program (35). In addition, a 2D ^{1}H–^{15}N HSQC spectrum of $(CUG)_{97}$ was recorded on a 600 MHz Varian ^{UNITY}*INOVA* liquid state NMR spectrometer.

RESULTS

Numerical

For obtaining ^{15}N dipolar correlation spectra in uniformly labelled RNA the efficacy of the RF pulse sequence given in Figure 1 was assessed via numerical calculations. To reduce computational time, a simplified four-spin dipolar network as shown in Figure 2 was considered. In these simulations we have monitored, as a function of the dipolar mixing time, the magnitude of longitudinal magnetization transferred to the cytosine nitrogen N3 (CN3) starting with z magnetization on guanine nitrogen N1 (GN1) at the beginning of the mixing period. These simulations were carried out over a range of GN1–CN3 dipolar coupling strengths D of 70–20 Hz, approximately corresponding to an N1–N3 distance range of 2.62–3.97 Å. As noted in our recent studies (36), dipolar recoupling dynamics with adiabatic inversion pulses is not significantly affected by the chemical shift, dipolar tensor orientational parameters or the magnitude of ^{15}N CSAs. Hence, numerical simulations were performed by considering only the typical ^{15}N isotropic chemical shifts of the relevant nuclei. Other relevant parameters employed in the simulations are given in the figure caption. Over an N–N dipolar coupling range of 50–70 Hz ($r_{NN} \approx$ 2.9–2.6 Å), 5–10% of the GN1 magnetization can be transferred to the spin CN3 employing dipolar mixing periods on the order of 15–20 ms (Fig. 2). An analysis of the recoupling dynamics at longer mixing times would require taking into consideration other N–N dipolar interactions that have been neglected in our simulations. Even with dipolar mixing periods of <20 ms, it is apparent from the simulations (see Fig. 2) that the magnitude of the transferred magnetization is sufficient to lead to cross-peaks of measurable intensities between the hydrogen-bonded nitrogen nuclei.

Experimental

The experimental assessment of the potential of ^{15}N MAS NMR for the study of large RNAs was performed on a uniformly ^{15}N-labelled sample of $(CUG)_{97}$ (Fig. 3A). The purity and fold of the $(CUG)_{97}$ were ascertained by gel electrophoresis (Fig. 3B) and by recording in the solution state a $^{1}H–^{15}N$ HSQC spectrum of the RNA sample. The RNA sample employed in the solution state NMR experiments had a concentration of 200 μM and was taken from the same preparation as used for the ssNMR experiments. Purified $(CUG)_{97}$ gives rise to only two cross-peaks in the solution state 2D correlation experiment (Fig. 3C). The ^{15}N resonance at 150 p.p.m. corresponds to the imino group of guanine and the resonance at 158 p.p.m. to the imino group of uridine, respectively. The observation of the two imino signals indicates slow exchange for the respective protons and hence the involvement of those groups in hydrogen bonds. This in turn indicates that the $(CUG)_{97}$ adopts double-stranded conformation through base pairing of its self-complementary sequence, as concluded earlier from biochemical studies (25,26). The repeating conformational unit of $(CUG)_{97}$ contains a mismatched UU base pair (37,38) flanked by canonical Watson–Crick pairs (Fig. 3A).

The MAS ^{15}N dipolar correlation spectra of the $(CUG)_{97}$ RNA sample were obtained with the RF pulse sequence shown in Figure 1. In these experiments a short cross-polarization (CP) contact time was used to selectively enhance ^{15}N signals arising from the imino and amino nitrogens. While the usage of CP contact times of the order of milliseconds generally leads to sensitivity enhancement of all the nitrogen sites, the short contact time used here permits suppression of signals from unprotonated nitrogens and reduces spectral overlap. Figure 4 shows the 1D CPMAS ^{15}N spectra of the RNA obtained employing CP contact times of 3.0 ms (Fig. 4A) and 175 μs (Fig. 4B). While all expected nitrogen signals are observed in the spectrum (Fig. 4A), those nitrogens that are proton attached are seen preferentially using a shorter cross-polarization time. This allows the imino and amino nitrogens to be distinguished from the other resonances. The indicated assignments are based on ^{15}N chemical shifts typically seen in solution state NMR (7) and are consistent with the 2D $^{1}H–^{15}N$ (Fig. 3C) and 2D $^{15}N–^{15}N$ (Fig. 5) correlation spectra. The ^{15}N dipolar correlation spectrum given in Figure 5 was obtained with the lyophylized and rehydrated RNA sample employing a dipolar mixing period of 20 ms. The canonical and reverse Watson–Crick GC base-pairing schemes are also indicated in Figure 5. To reduce spectral data acquisition time, the amino nitrogen resonances are folded in the ω_1 dimension. The short CP contact time (175 μs) employed leads to the asymmetric cross-peak distribution in the 2D spectrum. Starting with the imino and amino nitrogens, all correlation peaks arising from short-range N–N dipolar interactions are visible. The cross-peak between the imino nitrogen of guanine and the N3 nitrogen of cytosine can be clearly observed in the 2D spectrum. However, cross-peaks between GN1–GN9, GN1–GN7 and GN1–CN4 arising from long-range dipolar interactions were not observed. Besides the spectrum shown in Figure 5, we have also collected dipolar correlation data employing a shorter dipolar mixing time of 14.28 ms on the same RNA sample after dissolving and refreezing. Again the GC cross-peak was clearly detected (Fig. 6). It is noteworthy that both the lyophilized and rehydrated sample as well as the frozen sample generated spectra of similar quality.

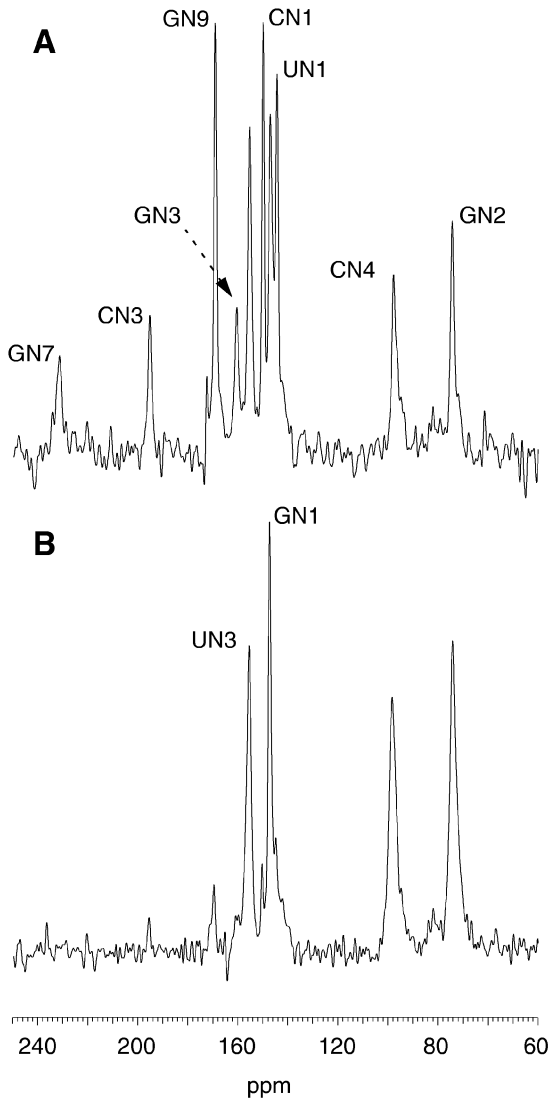

Figure 4. A ^{15}N CPMAS spectrum of the lyophylized and rehydrated RNA sample obtained at a spinning speed of 7000 Hz and temperature of approximately –15°C employing a data acquisition time of 20 ms with CP contact time of (**A**) 3 ms and (**B**) 175 μs. Spectra A and B were respectively collected employing a recycle time of 10 s and 2 s and with 1296 and 512 transients. The chemical shifts are referenced to liquid NH_3 assuming that solid NH_4Cl has a chemical shift of 38.5 p.p.m.

DISCUSSION

In a solution state HNN-COSY experiment, the identity of the acceptor nitrogen involved in NH...N hydrogen bonds is generally inferred either from the chemical shift of the acceptor nitrogen and/or via additional two-bond correlation experiments (12). On the other hand, in dipolar coupling-based broadband ssNMR the assignment of the acceptor nitrogen can be achieved by utilizing the presence of additional correlation peaks in the spectral data. Here, the

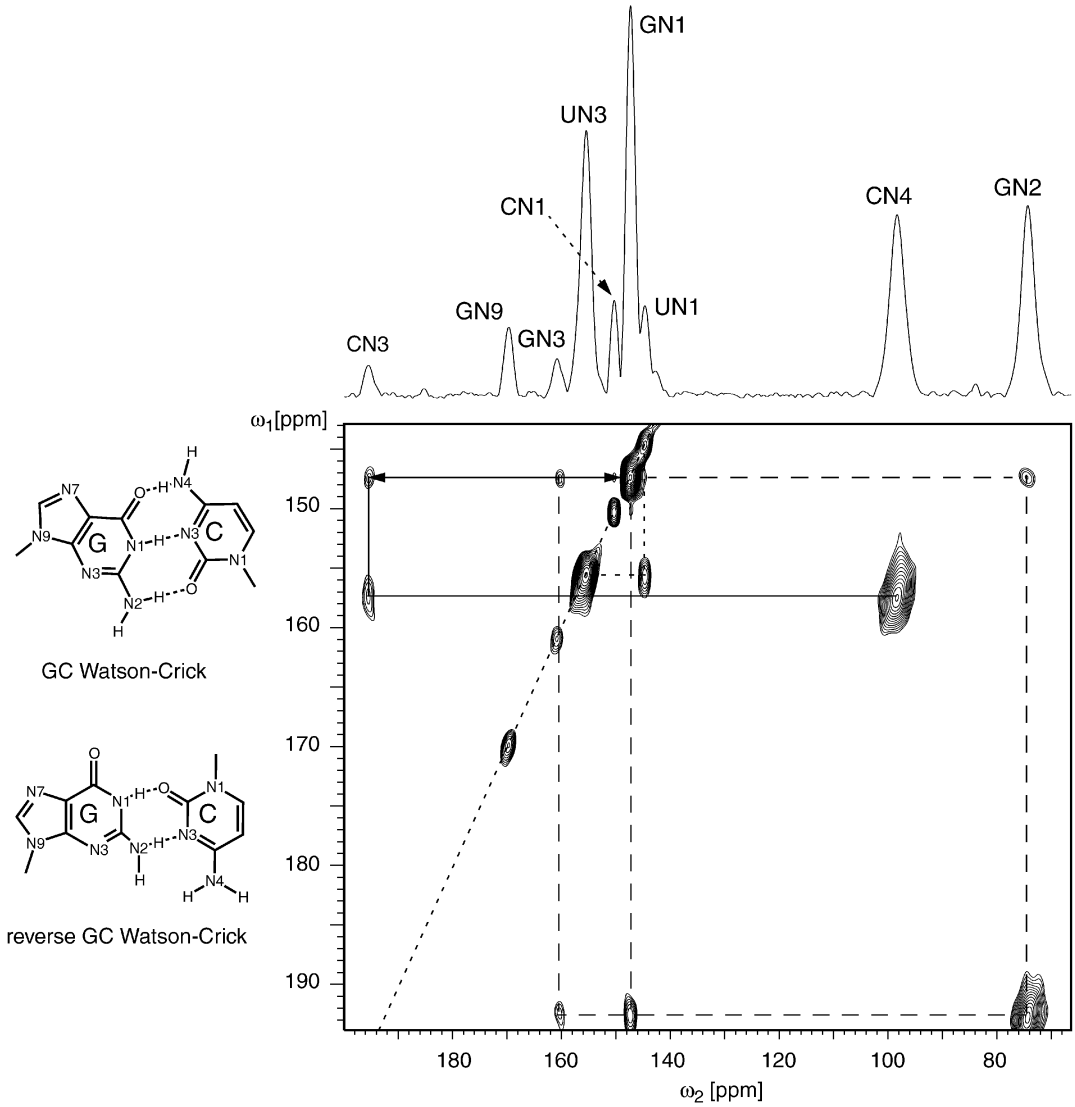

Figure 5. Experimental ^{15}N dipolar chemical shift correlation spectrum of the lyophylized and rehydrated RNA sample (zoomed plot) obtained at a spinning speed of 7000 Hz, with a data acquisition in the direct dimension of 10 ms, dipolar recoupling period of 20 ms, CP contact time of 175 µs, recycle time of 4.1 s, ω_1 spectral width of 3000 Hz and 32 t_1 increments with 512 transients per t_1 increment. The RF carrier was kept at 164.6 p.p.m.. The amino nitrogen lines are folded in the ω_1 dimension. Dipolar recoupling was effected by employing the [p5p7m4] phasing scheme with 'cagauss' adiabatic pulses (142 µs, 28.0 kHz γH_1, 50 kHz sweep width) (23,32) as implemented in the Varian Pbox pulse-shaping software. The assignments of the different resonances are indicated in the spectral projection given. Also illustrated are the normal and reverse GC Watson–Crick base-pairing schemes. The spectral diagonal is indicated by a dotted line.

presence of a cross-peak between the cytosine amino nitrogen and CN3 facilitates the identification of the acceptor nitrogen in the hydrogen bond involving the guanine imino donor ^{15}N nucleus. For $(CUG)_{97}$ RNA, the correlation peak between GN1 and CN3 suggests the presence of only a canonical GC Watson–Crick base-pairing scheme, as predicted by previous studies (25,26). A reverse GC Watson–Crick base-pairing scheme should lead to a correlation peak between the amino nitrogen of guanine and CN3, and such a correlation is not observed here. Although the intensity of the cross-peak between the donor and acceptor nitrogen nuclei in the GC base pair is not very high as expected from numerical simulations, it is sufficiently large to be clearly detected in the 2D dipolar correlation spectrum of uniformly ^{15}N-labelled $(CUG)_{97}$ where the GC cross-peak could arise in principle via either interstrand or intrastrand dipolar interactions. Molecular modelling studies predict an intrastrand GN1–CN3 distance of ~3.5 Å, corresponding to a dipolar coupling strength of <30 Hz. From numerical simulations, the contribution to the observed GC cross-peak intensity is much higher from interstrand than from intrastrand GC dipolar interactions. Also, for the mixing time employed, no intrabase cross-peaks between the nuclei GN1–GN7 ($r_{NN} \approx 3.62$ Å) and GN1–CN4 ($r_{NN} \approx 3.68$ Å) are detectable. Thus it is safe to conclude that the GC cross-peak in the 2D spectrum shown in Figure 5 reflects interstrand dipolar interactions. If required, additional MAS NMR experiments, such as the measurement of ^{15}N–^{1}H distances (39–42), can further validate the conclusions

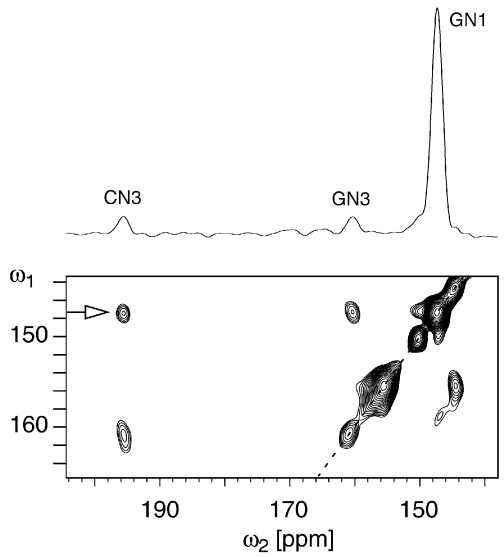

Figure 6. Experimental ^{15}N dipolar chemical shift correlation spectrum for the redissolved and frozen RNA sample (zoomed plot) obtained with a dipolar recoupling period of 14.28 ms, ω_1 spectral width of 3200 Hz and 32 t_1 increments with 640 transients per t_1 increment. Dipolar recoupling was effected by employing the [p5m4] phasing scheme. The spectral cross-section taken at the position indicated is also given at the top of the 2D spectrum. Other parameters employed were as in Figure 5. The spectral diagonal is indicated by a dotted line.

reached via ^{15}N dipolar correlation spectroscopy. In fact, information on all of the distances between the nuclei in the dipolar network ^{15}N–^{1}H...^{15}N would enable a full characterization of the hydrogen bond.

Recent studies carried out on simple model systems containing a pair of dipolar coupled ^{15}N nuclei suggest that it should be feasible to extract internuclear distances from adiabatic inversion pulse driven magnetization exchange experiments (36). Unlike the difficulties in obtaining long-range ^{13}C–^{13}C distances in uniformly ^{13}C-labelled samples (11), the measurement of ^{15}N–^{15}N distances in uniformly ^{15}N-labelled biological systems does not pose any problems owing to the absence of dipolar truncation effects (43,44). However, precise measurement of ^{15}N–^{15}N internuclear distances would require consideration of the effects of chemical shift anisotropy, chemical shift and dipolar tensor orientations as well as all relevant dipolar spin interactions and various relaxation processes. Additionally, quantitative distance measurements also require the usage of much lower temperatures for freezing local and global motions that scale down the strength of the dipolar interactions between nuclei significantly. Owing to hardware limitations, the experimental measurements presented here have been carried out only at a temperature of approximately –15°C. Precise measurement of ^{15}N–^{15}N distances would require an analysis of the initial cross-peak intensity build-up curves. However, for resonance assignment studies and for obtaining approximate internuclear distance constraints, as needed in distance geometry based structure calculations, such rigorous analysis of cross-peak intensity build-up curves is not necessary.

In conclusion, the results presented here demonstrate for the first time that ^{15}N MAS dipolar correlation experiments in uniformly ^{15}N-labelled RNA can be employed for probing the spatial proximity of nitrogen nuclei and hence for the possible presence of NH...N hydrogen bonds between complementary bases. The use of ^{15}N MAS ssNMR could enable rapid assessment of the base-paired regions in large RNAs, including tertiary interactions. However, this may require segment-, base- or strand-specific labelling strategies (45–49) to avoid spectral overlaps and the adoption of techniques designed to obtain improved signal-to-noise ratios (e.g. inverse detection) (50). In addition to the ^{15}N dipolar recoupling measurements reported here, ^{13}C dipolar recoupling experiments with ^{13}C labelled samples can be employed for the characterization of non-canonical base pairs which do not contain NH...N hydrogen bonds but are frequently involved in the intricate structures of biologically active RNA molecules. The encouraging results presented here suggest that it should be possible to structurally characterize the dsCUG RNA in more detail via MAS NMR, including its interaction with the muscleblind proteins. This will help to gain insight into the molecular basis of myotonic dystrophy.

ACKNOWLEDGEMENTS

The IMB is a member of the Science Association 'Gottfried Wilhelm Leibniz' (WGL) and is financially supported by the Federal Government of Germany and the State of Thuringia.

REFERENCES

1. Gesteland,R.F., Atkins,J.F. and Cech,T.R. (1999) *The RNA World* (2nd edn). Cold Spring Harbor Laboratory Press, Cold Spring Harbor, NY.
2. Ohlenschlager,O., Wohnert,J., Ramachandran,R., Sich,C. and Gorlach,M. (2003) Nuclear magnetic resonance studies of ribonucleic acids. *Spectroscopy*, **17**, 537–547.
3. Furtig,B., Richter,C., Wohnert,J. and Schwalbe,H. (2003) NMR spectroscopy of RNA. *Chembiochem*, **4**, 936–962.
4. Ohlenschlager,O., Wohnert,J., Bucci,E., Seitz,S., Hafner,S., Ramachandran,R., Zell,R. and Gorlach,M. (2004) The structure of the stemloop D subdomain of Coxsackievirus B3 cloverleaf RNA and its interaction with the proteinase 3C. *Structure*, in press.
5. Stoldt,M., Wohnert,J., Ohlenschlager,O., Gorlach,M. and Brown,L.R. (1999) The NMR structure of the 5S rRNA E-domain-protein L25 complex shows preformed and induced recognition. *EMBO J.*, **18**, 6508–6521.
6. Hermann,T. and Patel,D.J. (1999) Stitching together RNA tertiary architectures. *J. Mol. Biol.*, **294**, 829–849.
7. Wijmenga,S.S. and van Buuren,B.N.M. (1998) The use of NMR methods for conformational studies of nucleic acids. *Prog. Nucl. Magn. Reson. Spectrosc.*, **32**, 287–387.
8. Bennett,A.E., Griffin,R.G. and Vega,S. (1994) *Recoupling of Homo- and Heteronuclear Dipolar Interactions in Rotating Solids.* Springer, Berlin.
9. Griffin,R.G. (1998) Dipolar recoupling in MAS spectra of biological solids. *Nat. Struct. Biol.*, **5** (Suppl.), 508–512.
10. Dusold,S. and Sebald,A. (2000) Dipolar recoupling under magic-angle spinning conditions. *Annu. Rep. NMR Spectrosc.*, **41**, 185–264.
11. Castellani,F., van Rossum,B., Diehl,A., Schubert,M., Rehbein,K. and Oschkinat,H. (2002) Structure of a protein determined by solid-state magic-angle-spinning NMR spectroscopy. *Nature*, **420**, 98–102.
12. Dingley,A.J. and Grzesiek,S. (1998) Direct observation of hydrogen bonds in nucleic acid base pairs by internucleotide $^{2}J_{NN}$-couplings. *J. Am. Chem. Soc.*, **120**, 1601–1602.
13. Wohnert,J., Dingley,A.J., Stoldt,M., Gorlach,M., Grzesiek,S. and Brown,L.R. (1999) Direct identification of NH..N hydrogen bonds in non-canonical base pairs of RNA by NMR spectroscopy. *Nucleic Acids Res.*, **27**, 3104–3110.
14. Grzesiek,S., Cordier,F. and Dingley,A.J. (2001) Scalar couplings across hydrogen bonds. *Methods Enzymol.*, **338**, 111–133.

15. Bennett,A.E., Ok,J.H., Griffin,R.G. and Vega,S. (1992) Chemical shift correlation spectroscopy in rotating solids: Radio frequency-driven dipolar recoupling and longitudinal exchange. *J. Chem. Phys.*, **96**, 8624–8627.
16. Bennett,A.E., Rienstra,C.M., Griffith,J.M., Zhen,W., Lansbury,P.T. and Griffin,R.G. (1998) Homonuclear radio frequency-driven recoupling in rotating solids. *J. Chem. Phys.*, **108**, 9463–9479.
17. Boender,G.J., Raap,J., Prytulla,S., Oschkinat,H. and de Groot,H.J.M. (1995) MAS NMR structure refinement of uniformly ^{13}C enriched chlorophyll a/water aggregates with 2D dipolar correlation spectroscopy. *Chem. Phys. Lett.*, **237**, 502–508.
18. McDermott,A., Polenova,T., Bockmann,A., Zilm,K.W., Paulson,E.K., Martin,R.W., Montelione,G.T. and Paulsen,E.K. (2000) Partial NMR assignments for uniformly (^{13}C, ^{15}N)-enriched BPTI in the solid state. *J. Biomol. NMR*, **16**, 209–219.
19. Pauli,J., van Rossum,B., Forster,H., de Groot,H.J. and Oschkinat,H. (2000) Sample optimization and identification of signal patterns of amino acid side chains in 2D RFDR spectra of the alpha-spectrin SH3 domain. *J. Magn. Reson.*, **143**, 411–416.
20. Pauli,J., Baldus,M., van Rossum,B., de Groot,H. and Oschkinat,H. (2001) Backbone and side-chain ^{13}C and ^{15}N signal assignments of the alpha-spectrin SH3 domain by magic angle spinning solid-state NMR at 17.6 Tesla. *Chembiochem*, **2**, 272–281.
21. vanRossum,B.J., Schulten,E.A., Raap,J., Oschkinat,H. and de Groot,H.J. (2002) A 3-D structural model of solid self-assembled chlorophyll a/H(2)O from multispin labeling and MAS NMR 2-D dipolar correlation spectroscopy in high magnetic field. *J. Magn. Reson.*, **155**, 1–14.
22. Heise,B., Leppert,J., Ohlenschlager,O., Gorlach,M. and Ramachandran,R. (2002) Chemical shift correlation via RFDR: elimination of resonance offset effects. *J. Biomol. NMR*, **24**, 237–243.
23. Leppert,J., Heise,B., Ohlenschlager,O., Gorlach,M. and Ramachandran,R. (2003) Broadband RFDR with adiabatic inversion pulses. *J. Biomol. NMR*, **26**, 13–24.
24. Brook,J.D., McCurrach,M.E., Harley,H.G., Buckler,A.J., Church,D., Aburatani,H., Hunter,K., Stanton,V.P., Thirion,J.P., Hudson,T. *et al.* (1992) Molecular basis of myotonic dystrophy: expansion of a trinucleotide (CTG) repeat at the 3′ end of a transcript encoding a protein kinase family member. *Cell*, **68**, 799–808.
25. Napierala,M. and Krzyzosiak,W.J. (1997) CUG repeats present in myotonin kinase RNA form metastable 'slippery' hairpins. *J. Biol. Chem.*, **272**, 31079–31085.
26. Michalowski,S., Miller,J.W., Urbinati,C.R., Paliouras,M., Swanson,M.S. and Griffith,J. (1999) Visualization of double-stranded RNAs from the myotonic dystrophy protein kinase gene and interactions with CUG-binding protein. *Nucleic Acids Res.*, **27**, 3534–3542.
27. Kanadia,R.N., Johnstone,K.A., Mankodi,A., Lungu,C., Thornton,C.A., Esson,D., Timmers,A.M., Hauswirth,W.W. and Swanson,M.S. (2003) A muscleblind knockout model for myotonic dystrophy. *Science*, **302**, 1978–1980.
28. Miller,J.W., Urbinati,C.R., Teng-Umnuay,P., Stenberg,M.G., Byrne,B.J., Thornton,C.A. and Swanson,M.S. (2000) Recruitment of human muscleblind proteins to (CUG)(n) expansions associated with myotonic dystrophy. *EMBO J.*, **19**, 4439–4448.
29. Charlet,B.N., Savkur,R.S., Singh,G., Philips,A.V., Grice,E.A. and Cooper,T.A. (2002) Loss of the muscle-specific chloride channel in type 1 myotonic dystrophy due to misregulated alternative splicing. *Mol. Cells*, **10**, 45–53.
30. Mankodi,A., Takahashi,M.P., Jiang,H., Beck,C.L., Bowers,W.J., Moxley,R.T., Cannon,S.C. and Thornton,C.A. (2002) Expanded CUG repeats trigger aberrant splicing of ClC-1 chloride channel pre-mRNA and hyperexcitability of skeletal muscle in myotonic dystrophy. *Mol. Cells*, **10**, 35–44.
31. Sambrook,J., Fritsch,E.F. and Maniatis,T. (1989) *Molecular Cloning: A Laboratory Manual* (2nd edn). Cold Spring Harbor Laboratory Press, Cold Spring Harbor, NY.
32. Kupce,E. and Freeman,R. (1996) Optimized adiabatic pulses for wideband spin inversion. *J. Magn. Reson.*, **A118**, 299–303.
33. Tycko,R., Pines,A. and Guckenheimer,J. (1985) Fixed point theory of iterative excitation schemes in NMR. *J. Chem. Phys.*, **83**, 2775–2802.
34. Levitt,M.H., Freeman,R. and Frenkiel,T. (1983) Broadband decoupling in high-resolution nuclear magnetic resonance spectroscopy. *Adv. Magn. Reson.*, **11**, 47–110.
35. Bak,M., Rasmussen,J.T. and Nielsen,N.C. (2000) SIMPSON: a general simulation program for solid-state NMR spectroscopy. *J. Magn. Reson.*, **147**, 296–330.
36. Leppert,J., Ohlenschlager,O., Gorlach,M. and Ramachandran,R. (2004) RFDR with adiabatic pulses: application to internuclear distance measurements. *J. Biomol. NMR*, **28**, 229–233.
37. Ban,N., Nissen,P., Hansen,J., Moore,P.B. and Steitz,T.A. (2000) The complete atomic structure of the large ribosomal subunit at 2.4 Å resolution. *Science*, **289**, 905–920.
38. Wang,Y.X., Huang,S. and Draper,D.E. (1996) Structure of a U.U pair within a conserved ribosomal RNA hairpin. *Nucleic Acids Res.*, **24**, 2666–2672.
39. DiVerdi,J.A. and Opella,S.J. (1982) N-H bond lengths in DNA. *J. Am. Chem. Soc.*, **104**, 1761–1762.
40. Roberts,J.E., Harbison,G.S., Munowitz,M.G., Herzfeld,J. and Griffin,R.G. (1987) Measurement of heteronuclear bond distances in polycrystalline solids by solid state NMR techniques. *J. Am. Chem. Soc.*, **109**, 4163–4169.
41. Howhy,M., Jaroniec,C.P., Reif,B., Rienstra,C.M. and Griffin,R.G. (2000) Local structure and relaxation in solid state NMR: accurate measurement of amide N–H bond length and H–N–H bond angles. *J. Am. Chem. Soc.*, **122**, 3218–3219.
42. Zhao,X., Sudmeier,J.L., Bachovchin,W.W. and Levitt,M.H. (2001) Measurement of NH bond lengths by fast magic-angle spinning solid-state NMR spectroscopy: a new method for the quantification of hydrogen bonds. *J. Am. Chem. Soc.*, **123**, 11097–11098.
43. Hodgkinson,P. and Emsley,L. (1999) The accuracy of distance measurements in solid-state NMR. *J. Magn. Reson.*, **139**, 46–59.
44. Kiihne,S.R., Geahigan,K.B., Oyler,N.A., Zebroski,H., Mehta,M.A. and Drobny,G.P. (1999) Distance measurements in multiply labeled crystalline cytidines by dipolar recoupling solid state NMR. *J. Phys. Chem.*, **A103**, 3890–3903.
45. Batey,R.T., Inada,M., Kujawinski,E., Puglisi,J.D. and Williamson,J.R. (1992) Preparation of isotopically labeled ribonucleotides for multidimensional NMR spectroscopy of RNA. *Nucleic Acids Res.*, **20**, 4515–4523.
46. SantaLucia,J., Jr, Shen,L.X., Cai,Z., Lewis,H. and Tinoco,I., Jr (1995) Synthesis and NMR of RNA with selective isotopic enrichment in the bases. *Nucleic Acids Res.*, **23**, 4913–4921.
47. Xu,J., Lapham,J. and Crothers,D.M. (1996) Determining RNA solution structure by segmental isotopic labeling and NMR: application to *Caenorhabditis elegans* spliced leader RNA 1. *Proc. Natl Acad. Sci. USA*, **93**, 44–48.
48. Dieckmann,T. and Feigon,J. (1997) Assignment methodology for larger RNA oligonucleotides: application to an ATP-binding RNA aptamer. *J. Biomol. NMR*, **9**, 259–272.
49. Kim,I., Lukavsky,P.J. and Puglisi,J.D. (2002) NMR study of 100 kDa HCV IRES RNA using segmental isotope labeling. *J. Am. Chem. Soc.*, **124**, 9338–9339.
50. Chevelkov,V., van Rossum,B.J., Castellani,F., Rehbein,K., Diehl,A., Hohwy,M., Steuernagel,S., Engelke,F., Oschkinat,H. and Reif,B. (2003) ^{1}H detection in MAS solid-state NMR spectroscopy of biomacromolecules employing pulsed field gradients for residual solvent suppression. *J. Am. Chem. Soc.*, **125**, 7788–7789.